

# Intermolecular Interactions of Brush-Like Polymers

Yo NAKAMURA<sup>†</sup>

*Department of Polymer Chemistry, Kyoto University, Katsura, Kyoto 615-8510,  
Japan*

<sup>†</sup> To whom correspondence should be addressed (E-mail: [yonaka@molsci.polym.kyoto-u.ac.jp](mailto:yonaka@molsci.polym.kyoto-u.ac.jp))

RUNNING HEAD: Intermolecular Interactions of Brush-Like Polymers

The excluded-volume parameter  $B$  for brush-like polymers is calculated assuming that each brush-like segment is consisting of a straight main chain with Gaussian side chains. Interactions between brush-like segments were represented by the binary and ternary interactions among side-chain segments. The leading term for the perturbation calculation in terms of the binary interaction between side-chain segments gave much larger  $B$  than the experimental values, which were determined from analyses of the second virial coefficient  $A_2$  of polystyrene polymacromonomers in toluene, suggesting that consideration of higher terms is necessary. Results based on the smoothed-density (SD) model gave much closer values to the experimental values. Perturbation calculation considering the ternary interactions among side-chain segments revealed that consideration of residual ternary interactions is necessary for theta solvent systems. This is rather contradicting to the experimental results that  $A_2$  for polystyrene polymacromonomers in cyclohexane vanishes at 34.5 °C. However, the calculated results based on the SD model showed that the contribution from these effects is within the experimental error.

**Keywords:** brush-like polymers; second virial coefficient; cluster integrals; excluded-volume effect; polymacromonomer;

## INTRODUCTION

Comb-branched polymers with dense side chains are called brush-like polymers.<sup>1-3</sup> After the establishment of synthesis routes, number of studies on such polymers increased because of their curious properties, such as liquid crystal formations.<sup>4-6</sup> A typical method to obtain brush-like polymers is polymerization of macromonomers,<sup>7,8</sup> which are consisting of linear polymers with a polymerizable group at one end of the chain. From solution studies of polymacromonomers in solution, it was shown that these molecules behave as stiff chains.<sup>1,2,9-14</sup>

We have studied dimensional properties of polymacromonomers consisting of polystyrene (PS) in a good (toluene at 15.0°C) and a theta (cyclohexane at 34.5°C) solvents and determined the stiffness parameter  $\lambda^{-1}$  as functions of the degree of polymerization of side chain  $n_s$ .<sup>11-13,15-18</sup> The  $\lambda^{-1}$  values obtained for these polymers were explained by the first-order perturbation calculation in terms of segmental interactions among side chains.<sup>19</sup> It was also shown that polymacromonomer chains in the good solvent are expanded by intramolecular excluded-volume effects,<sup>12,13</sup> when the main chain is sufficiently long comparing with the Kuhn segment length or  $\lambda^{-1}$ . The magnitude of these effects are quantified by the excluded-volume parameter  $B$ ,<sup>20,21</sup> which represents the excluded volume of a pair of segments divided by the square of the segment length. The  $B$  values, obtained from the radius expansion factor, were found to increase with the side chain length. The interaction between polymacromonomer segments may be described as a sum of segmental interactions among side-chains.

In the calculation of  $\lambda^{-1}$  for brush-like polymers, we modeled the polymer molecule by a wormlike main chain with Gaussian side chains.<sup>19</sup> The essentially same model, i.e. a straight main chain with Gaussian side chains, may be used for the brush-like segment, which is an interacting unit of brush-like polymers. Interactions between two brush-like segments may be described by a sum of the interactions

among side chain beads. Since two side chains belong to different brush-like segments contact at a place apart from the main chains, interactions between these segments can be regarded as long-ranged. Thus, the problem is similar to segment-segment interactions of polyelectrolytes.<sup>22</sup>

The interaction between segments are also reflected by the second virial coefficient  $A_2$ . Here, we analyze previously obtained data for  $A_2$  of PS polymacromonomers in toluene<sup>11,15,18</sup> to determine  $B$  values for different side chain lengths. Those values for  $B$  obtained are compared with the theoretical results based on the perturbation and the smoothed-density (SD) methods.

## THEORIES

### Basic Equations

The brush-like segment is modeled by a straight main chain of the length  $a$  with Gaussian side chains connected to it at intervals of  $h_s$ . Each side chain is consisting of  $n_s$  beads connected by bonds of length  $b$ .

The excluded volume for a pair of brush-like segments may be given by<sup>22</sup>

$$v = \int \langle 1 - e^{-W_{12}(\mathbf{r})/k_B T} \rangle d\mathbf{r} \quad (1)$$

We note that the inter-segment potential  $W_{12}(\mathbf{r})$  depends on the direction of the main chains of these segments as well as the distance  $\mathbf{r}$  between the middle points of the main chains. The angular brackets of the above equation mean averaging over the relative direction of these segments. The excluded-volume parameter  $B$  is defined by

$$B = v/a^2 \quad (2)$$

The distance and directions of two brush-like segments are illustrated in Figure 1. The first brush-like segment (segment 1) is assumed to lie along the  $z$ -axis of the Cartesian coordinate with its center of mass at the origin O. The side chains are numbered from 1 to  $a/2h_s$  from the one closest to the origin for positive  $z$  and from

$-1$  to  $-a/2h_s$  for negative  $z$ . The side chain beads (or segments) are numbered from 1 to  $n_s$  from the closest one to the main chain. Here, the number of side chains in one segment  $a/h_s$  and  $n_s$  are considered to be much larger than 1. The position of the center of the main chain of the second brush-like segment (segment 2) is represented by  $\mathbf{r}$ . The direction of the segment 2 may be represented based on the other Cartesian coordinate  $(x', y', z')$  with its origin fixed at the center of the segment 2 and with each axis being parallel to the first Cartesian coordinate. The azimuthal and rotational angles around the  $z'$  axis are represented by  $\theta$  and  $\phi$ , respectively. The ways of numbering side chains and side-chain beads of the segment 2 are taken to be the same as those of the segment 1.

⟨ Figure 1 ⟩

The probability that the  $p_i$ th bead of the  $i$ th side chain of the segment 1 lies between  $\mathbf{R}$  and  $\mathbf{R} + d\mathbf{R}$  may be given by the following Gaussian function

$$P(\mathbf{R}; \mathbf{r}_i, p_i) d\mathbf{R} = \left( \frac{3}{2\pi b^2} \right)^{3/2} \exp \left[ -\frac{3(\mathbf{R} - \mathbf{r}_i)^2}{2p_i b^2} \right] d\mathbf{R} \quad (3)$$

Here,  $\mathbf{r}_i$  represents the position of the connecting point of the  $i$ th side chain to the main chain. A similar expression for  $P(\mathbf{R}; \mathbf{r}_j, q_j)$  for the the  $q_j$ th bead of the  $j$ th side chain of the segment 2 can be obtained, where  $\mathbf{r}_j$  represents the distance from the origin O to the connecting point of the  $j$ th side chain to the main chain of the segment 2.

The probability density that two segments  $p_i$  and  $q_j$  are in contact can be calculated as<sup>19</sup>

$$\begin{aligned} P(\mathbf{0}_{p_i q_j}; \mathbf{r}_{ij}, p_i, q_j) &= \int P(\mathbf{R}; \mathbf{r}_i, p_i) P(\mathbf{R}; \mathbf{r}_j, q_j) d\mathbf{R} \\ &= \left( \frac{3}{2\pi b^2} \right)^{3/2} \frac{1}{(p_i + q_j)^{3/2}} \exp \left[ -\frac{3r_{ij}^2}{2b^2(p_i + q_j)} \right] \end{aligned} \quad (4)$$

Here,  $\mathbf{r}_{ij} = \mathbf{r}_j - \mathbf{r}_i$  and  $\mathbf{0}_{p_i q_j}$  means that the distance between the segments  $p_i$  and  $q_j$  is zero. We note that  $\mathbf{r}_i$  and  $\mathbf{r}_j - \mathbf{r}$  can be written as follows:

$$\begin{aligned}\mathbf{r}_i &= (0, 0, ih_s) \\ \mathbf{r}_j - \mathbf{r} &= (jh_s \sin \theta \cos \phi, jh_s \sin \theta \sin \phi, jh_s \cos \theta)\end{aligned}$$

Thus,  $\mathbf{r}_{ij}$  is a function of  $\mathbf{r}$ ,  $i$ ,  $j$ ,  $\theta$ , and  $\phi$ , although we do not indicate for clarity.

### Binary-Cluster Approximation

*Perturbation Calculation.* The potential for two brush-like segments  $W_{12}(\mathbf{r})$  may be expressed by the sum of the pair potentials  $w(\mathbf{u}_{p_i q_j})$  between segments  $p_i$  and  $q_j$ , separated by  $\mathbf{u}_{p_i q_j}$ .

$$W_{12}(\mathbf{r}) = \sum_{i,j} \sum_{p_i, q_j} w(\mathbf{u}_{p_i q_j}) \quad (5)$$

Introducing the following function,

$$\chi_{p_i q_j} = e^{-w(\mathbf{u}_{p_i q_j})/k_B T} - 1 \quad (6)$$

1 can be expanded as<sup>23</sup>

$$v = \sum_{i,j} \sum_{p_i, q_j} \int \langle \chi_{p_i q_j} \rangle d\mathbf{r} + \sum_{i,j,k} \sum_{p_i, q_j, s_k} \int \langle \chi_{p_i q_j} \chi_{p_i s_k} \rangle d\mathbf{r} + \dots \quad (7)$$

Assuming the short range interaction between segments,  $\chi_{p_i q_j}$  may be replaced by  $-\beta_2 \delta(\mathbf{u}_{p_i q_j})$  with the delta function, where  $\beta_2$  means the binary cluster integral between side-chain beads. Then, the first term of the right-hand side of 7, designated by  $v_{2-1}$ , can be written as

$$v_{2-1} = \beta_2 \sum_{i,j} \sum_{p_i, q_j} \left\langle \int P(\mathbf{0}_{p_i q_j}; \mathbf{r}_{ij}, p_i, q_j) d\mathbf{r} \right\rangle \quad (8)$$

Substituting 4 into the above equation, we obtain

$$v_{2-1} = \left( \frac{n_s a}{h_s} \right)^2 \beta_2 \quad (9)$$

This is an obvious result, because  $(n_s a/h_s)^2$  represents the total number of cases that one bead of the segment 1 and another bead of the segment 2 are in contact as shown in 2-1 of Figure 2.

⟨ Figure 2 ⟩

We also calculated the second term of the right-hand side of 7. However, it was found that the value of the second term is more than ten times as large as the first term, showing that the convergence of the power series is not good. Some discussions about this will be given in Conclusions.

*Smoothed-Density Model.* Since the convergence of the perturbation calculation was not good, we calculate  $v$  according to the smoothed-density (SD) model. In this model, the inter-segment potential is written as<sup>23</sup>

$$\frac{W_{12}(\mathbf{r})}{k_B T} = \beta_2 \sum_{i,j} \sum_{p_i, q_j} P(\mathbf{0}_{p_i, q_j}; \mathbf{r}_{ij}, p_i, q_j) \quad (10)$$

Substituting the above equation with 4 into 1, the excluded volume  $v_2^{\text{SD}}$  for this model is given by

$$v_2^{\text{SD}} = \int \left\langle 1 - \exp \left\{ -\beta_2 \sum_{i,j} \sum_{p_i, q_j} \left( \frac{3}{2\pi b^2} \right)^{3/2} \frac{1}{(p_i + q_j)^{3/2}} \exp \left[ -\frac{3r_{ij}^2}{2b^2(p_i + q_j)} \right] \right\} \right\rangle d\mathbf{r} \quad (11)$$

The sums over  $i$  and  $j$  may be approximated by integrals from  $-\infty$  to  $\infty$ . Further, we make the following assumption according to Fixman and Skolnick.<sup>22</sup> In Figure 1, we may denote the plain which is parallel to the  $z$ -axis and contains the main chain of the segment 2 as S. Assuming that the interaction between two brush-like segments occurs only when the projection of the main chain of the segment 2 onto

the  $xy$  plain crosses the perpendicular from the origin O to the plain S, we obtain

$$v_2^{\text{SD}} = a^2 \int_0^\infty du \int_0^\pi d\theta \sin^2 \theta \left\{ 1 - \exp \left[ -\beta_2 \left( \frac{3}{2\pi b^2} \right)^{1/2} \frac{1}{h_s^2 \sin \theta} \sum_{p_i, q_j} \frac{1}{(p_i + q_j)^{1/2}} \right. \right. \\ \left. \left. \times \exp \left( -\frac{3}{2b^2(p_i + q_j)} u^2 \right) \right] \right\} \quad (12)$$

Here,  $u$  represents the distance between the origin and the plain S. We obtained  $v_2^{\text{SD}}$  by numerical integration over  $u$  and  $\theta$  after summing over  $p_i$  and  $q_j$ .

### Effects of Ternary Clustering

*Perturbation Calculation.* It is known that ternary-cluster terms are not negligibly small at and near the theta point as the result that the binary-cluster integral reduces to the same order of the ternary-cluster integral.<sup>24</sup>

Here, we consider two ternary-clustering terms. One is for the case that two beads of a side chain belonging to segment 1 and one bead of a side chain belonging to segment 2 contact, as shown in 3-1 of Figure 2, where the former side chain makes a loop. The term for this case may be written as

$$v_{3-1} = 2\beta_3 \sum_{i,j} \sum_{p_i, q_i, s_j} \left\langle \int P(\mathbf{0}_{p_i q_i}, \mathbf{0}_{p_i s_j}; \mathbf{r}_{ij}, p_i, q_i, s_j) d\mathbf{r} \right\rangle \quad (13)$$

Here, the side chains  $i$  and  $j$  belong to the segment 1 and 2, respectively. The segments  $p_i$  and  $q_i$  are on the side chain  $i$  and the segment  $s_j$  is on the side chain  $j$ . The factor 2 comes from the two cases that the side chain making a loop belongs to the segment 1 or 2. The probability density in 13 is obtained with the aid of the Wang-Uhlenbeck theory<sup>23,25</sup> as

$$P(\mathbf{0}_{p_i q_i}, \mathbf{0}_{p_i s_j}; \mathbf{r}_{ij}, p_i, q_i, s_j) = \left( \frac{3}{2\pi b^2} \right)^3 \frac{1}{(q_i - p_i)^{3/2} (p_i + s_j)^{3/2}} \\ \times \exp \left[ -\frac{3r_{ij}^2}{2b^2(p_i + q_i)} \right] \quad (14)$$

The sums in 13 over  $p_i$ ,  $q_i$ , and  $s_j$  may be substituted into integrals from 0 to  $n_s$  and those over  $i$  and  $j$  may be substituted by integrations from  $-\infty$  to  $\infty$ . After



performing these integrations along with those on  $\mathbf{r}$ ,  $\theta$ , and  $\phi$ , we obtain

$$v_{3-1} = \frac{4a^2 n_s^2}{h_s^2} \left( \frac{3}{2\pi b^2} \right)^{3/2} \left( \frac{1}{\sigma^{1/2}} - \frac{2}{n_s^{1/2}} \right) \beta_3 \quad (15)$$

Here,  $\sigma$  means the minimum number of segments for making a loop. If we combine  $v_{3-1}$  with  $v_{2-1}$ , we obtain

$$v_{2-1} + v_{3-1} = \left( \frac{n_s a}{h_s} \right)^2 \left[ \beta_2 + 4 \left( \frac{3}{2\pi b^2} \right)^{3/2} \left( \frac{1}{\sigma^{1/2}} - \frac{2}{n_s^{1/2}} \right) \beta_3 \right] \quad (16)$$

The expression in the brackets of the above equation is the same as that appears in the second virial coefficient of linear polymers.<sup>24,26</sup> It is known that the negative  $\beta_2$  and the positive  $\beta_3$  terms considered to cancel out at the theta point, where  $A_2$  becomes zero, by

$$\beta_2 + \frac{4}{\sigma^{1/2}} \left( \frac{3}{2\pi b^2} \right)^{3/2} \beta_3 = 0$$

Thus, we can expect that the contribution from  $v_{2-1} + v_{3-1}$  to  $B$  vanishes at this point for sufficiently large  $n_s$ .

Next, we consider the case that two beads belonging to different side chains of segment 1 and one bead belonging to a side chain of the segment 2 contact. The term for this case, which is represented by 3-2 of Figure 2, may be written as

$$v_{3-2} = 2\beta_3 \sum_{i,j,k} \sum_{p_i, q_j, s_k} \left\langle \int P(\mathbf{0}_{p_i s_k}, \mathbf{0}_{q_j s_k}; \mathbf{r}_{ik}, \mathbf{r}_{ij}, p_i, q_j, s_k) d\mathbf{r} \right\rangle \quad (17)$$

Here, the side chains  $i$  and  $j$  belong to the segment 1 and the side chain  $k$  to the segment 2. The factor 2 appears from the same reason as 13. The probability density for this case can be written as

$$P(\mathbf{0}_{p_i q_j}, \mathbf{0}_{p_i s_k}; \mathbf{r}_{ik}, \mathbf{r}_{ij}, p_i, q_j, s_k) = \left( \frac{3}{2\pi b^2} \right)^3 \frac{1}{(p_i q_j + q_j s_k + p_i s_k)^{3/2}} \\ \times \exp \left\{ -\frac{3}{2b^2(p_i q_j + q_j s_k + p_i s_k)} [q_j r_{ik}^2 + p_i r_{ij}^2 + s_k h^2 (j-i)^2] \right\} \quad (18)$$

Substituting 18 into 17, we obtain

$$v_{3-2} = (4 \ln 2) \frac{n_s^2 a^2}{h_s^3} \beta_3 \quad (19)$$

Here, all the summations were approximated by integrals.

*Smoothed-Density Model.* The contribution of the ternary-clustering to  $v$  may also be calculated by the SD model. If we consider interactions of three beads belonging to different side chains, the potential for segments 1 and 2 may be given by

$$\frac{W_{12}(\mathbf{r})}{k_{\text{B}}T} = \beta_3 \sum_{i,j,k} \sum_{p_i,q_j,s_k} P(\mathbf{0}_{p_i q_j}, \mathbf{0}_{p_i s_k}; \mathbf{r}_{ik}, \mathbf{r}_{ij}, p_i, q_j, s_k) \quad (20)$$

From the similar argument to that for the SD model in the binary-cluster approximation, we obtain

$$v_3^{\text{SD}} = 2a^2 \int_0^\infty du \int_0^\pi d\theta \sin^2 \theta \left\{ 1 - \exp \left[ -\beta_3 \left( \frac{3}{2\pi b^2} \right)^{3/2} \frac{1}{h_s^3 \sin \theta} \sum_{p_i,q_j,s_k} \right. \right. \\ \left. \left. \times \frac{1}{[(p_i q_j + q_j s_k + p_i s_k)(p_i + q_j)]^{1/2}} \exp \left( -\frac{3(p_i + q_j)}{2b^2(p_i q_j + q_j s_k + p_i s_k)} u^2 \right) \right] \right\} \quad (21)$$

Here, we have multiplied the right-hand side of the above equation by 2 from the same reason of 17.

## COMPARISON WITH EXPERIMENTS

### Good Solvent Systems

Previous  $A_2$  data for PS polymacromonomers with different side chain length in toluene at 15.0°C<sup>12,15,18</sup> are plotted against the weight average molecular weight  $M_w$  in Figure 3. Here, F15, F33, F65, and F110 represent polymacromonomers consisting from side chains with 15, 33, 65, and 113 styrene residues. It is seen that  $A_2$  decreases with  $M_w$  and that the slope becomes steeper with increasing side chain length.

⟨ Figure 3 ⟩

These data may be explained by the following equation for the wormlike chain,<sup>27</sup>

$$A_2 = A_2^0 + A_2^{(\text{E})} \quad (22)$$

Here,  $A_2^0$  represents the term without the contribution of the chain-end effect and may be calculated from the following equation for the wormlike chain<sup>21</sup>

$$A_2^0 = \frac{N_A L^2 B}{2M^2} h(\lambda B, \lambda L) \quad (23)$$

where  $N_A$ ,  $L$ , and  $M$  denote the Avogadro constant, the contour length of the polymacromonomer molecule, and molecular weight, respectively. The last two parameters can be related by  $L = M/M_L$  with the molecular weight per unit contour length  $M_L$ . The dimensionless  $h(\lambda B, \lambda L)$  may be calculated from the modified Barrett equation<sup>27,28</sup> (see ref 21).

The term  $A_2^{(E)}$  for the chain-end effects may be expressed as<sup>27</sup>

$$A_2^{(E)} = a_{2,1} M^{-1} + a_{2,2} M^{-2} \quad (24)$$

Here,  $a_{2,1}$  and  $a_{2,2}$  are constants. The second term of the right-hand side of 24 is neglected here.

We determined  $B$  and  $a_{2,1}$  by fitting calculated curves to the data points as is illustrated by the solid lines in Figure 3. Here, we used known values of  $\lambda^{-1}$  and  $M_L$  for each sample<sup>12,15,18</sup> and  $h_s = 0.26$  nm, the averaged value for these samples,<sup>12,15,18</sup> along with  $\beta_2 = 0.034$  nm<sup>3</sup> for linear PS in toluene at 15.0°C<sup>29</sup> and  $b = 0.74$  nm determined from the unperturbed dimension of PS in cyclohexane at 34.5°C.<sup>30</sup> The resulted values are summarized in Table 1. Figure 4 shows the plots of  $B$  thus determined against  $n_s$ . The values obtained from the current analyses are close to those determined from  $\langle S^2 \rangle$ .

⟨ Table 1 ⟩

⟨ Figure 4 ⟩

The dashed line in Figure 4 represents the calculated values from 9. It is seen that they are much larger than the experimental values. The calculated values from

the SD model are much closer, but still larger than the experimental values by 10 - 50%. This may be ascribed to the approximated smoothed-density potential.

### Theta Solvent Systems

In Table 2, calculated  $B$  values from  $v_{2-1}$  and  $v_2^{\text{SD}}$  according to 19 and 21, respectively, are summarized. Here, we used  $\beta_3 = 0.004 \text{ nm}^3$  determined from the third virial coefficients of linear PS in cyclohexane at  $34.5^\circ\text{C}$ .<sup>24</sup> It is seen that the values from the perturbation calculation are much larger than those for the SD model. We may calculate the maximum values of  $A_2$  from 23 with  $h(\lambda B, \lambda L) = 1$ , if we ignore the chain-end effect. The  $A_2$  values obtained with  $B$  based on the SD model were less than  $3 \times 10^{-5} \text{ cm}^3 \text{ mol g}^{-2}$ , except for F15. From our previous results, the absolute values of  $A_2$  for PS polymacromonomers in cyclohexane were less than  $3 \times 10^{-5} \text{ cm}^3 \text{ mol g}^{-2}$  at the theta temperature ( $34.5^\circ\text{C}$ ) irrespective of molecular weight.<sup>11,15,18</sup> Thus, we may regard the calculated values for F33, F65, and F110 by the SD model agree with the experimental results. The value for F15 was about  $9 \times 10^{-5} \text{ cm}^3 \text{ mol g}^{-2}$ , which is rather larger than the experimental values.<sup>11</sup> This suggests necessity of consideration of some other interactions, effects from chain-ends or ternary-clustering of brush-like segments. The first-order perturbation calculations gave much larger  $A_2$  values (order of  $10^{-4} \text{ cm}^3 \text{ mol g}^{-2}$ ) than those from the SD model, showing the importance of the closed form.

⟨ Table 2 ⟩

### CONCLUSIONS

In this study, theoretical studies of  $B$  for brush-like polymers in good and theta solvents were carried out. It was shown that the SD-model calculations gave closer values to the experimental ones both in good and theta solvent systems if binary and ternary interactions among side chain beads were taken into consideration. The first-order perturbation calculation of  $B$  gave much larger values than observed ones,

being similar to the zeroth-order approximation of  $A_2$  for linear flexible polymers.<sup>23</sup> The calculated value for  $\beta_2^2$  term of  $B$  was much larger than the  $\beta_2$  term, showing that the convergence of the power series in terms of  $\beta_2$  is not good. The  $\beta_2^2$  terms for  $B$  arise from the double interactions between side chain beads belonging to different brush-like segments. Such higher-order interactions are considered to occur frequently when brush-like segments in almost parallel configuration approach each other. For the same reason, the SD model calculation with  $\beta_3$  interactions gave much closer values to the experimental ones for theta solvent systems than the first-order perturbation calculation. However, those values still deviate from experimental values. To obtain quantitative agreements, Monte Carlo calculations of  $B$  for the brush-like segments may be desirable.

## ACKNOWLEDGEMENTS

The author thanks Professor Takenao Yoshizaki of Kyoto University for valuable discussions. This research was financially supported by a Grant-in-Aid (22550111) from the Ministry of Education, Culture, Sports and Technology, Japan.

- 
- (1) Wintermantel, M., Schmidt, M., Tsukahara, Y., Kajiwara, K. & Kohjiya, S. Rodlike combs. *Macromol. Rapid Commun.* **15**, 279–284 (1994).
  - (2) Wintermantel, M., Fischer, K., Gerle, M., Ries, R., Schmidt, M., Kajiwara, K., Urakawa, H. & Wataoka, I. Lyotropic phases formed by molecular bottlebrushes. *Angew. Chem. Int. Ed. Engl.* **34**, 1472–1474 (1995).
  - (3) Nakamura, Y. & Norisuye, T. Brush-like polymers. in *Soft Matter Characterization* (eds. Borsali, R. & Pecora, R. ) Ch 5 (Springer Science+Business Media, LLC, New York 2008).

- (4) Tsukahara, Y., Ohta, Y. & Senoo, K. Liquid crystal formation of multibranched polystyrene induced by molecular anisotropy associated with its high branch density. *Polymer* **36**, 3413–3416 (1995).
- (5) Wintermantel, M., Gerle, M., Fischer, K., Schmidt, M., Wataoka, I., Urakawa, H., Kajiwara, K. & Tsukahara, Y. Molecular bottlebrushes. *Macromolecules* **29**, 978–983 (1996).
- (6) Nakamura, Y., Koori, M., Li, Y. & Norisuye, T. Lyotropic liquid crystal formation of polystyrene polymacromonomers in dichloromethane. *Polymer* **49**, 4877–4881 (2008).
- (7) Tsukahara, Y., Mizuno, K., Segawa, A. & Yamashita, Y. Study on the radical polymerization behavior of macromonomers. *Macromolecules* **22**, 1546–1552 (1989).
- (8) Tsukahara, Y., Tsutsumi, K., Yamashita, Y. & Shimada, S. Radical polymerization behavior of macromonomer 2. *Macromolecules* **23**, 5201–5208 (1990).
- (9) Nemoto, N., Nagai, M., Koike, A. & Okada, S. Diffusion and sedimentation studies of poly(macromonomer) in dilute solution. *Macromolecules* **28**, 3854–3859 (1995).
- (10) Kawaguchi, S., Akaike, K., Zhang, Z.-M., Matsumoto, H. & Ito, K. Water soluble bottlebrushes. *Polym. J.* **30**, 1004–1007 (1998).
- (11) Terao, K., Takeo, Y., Tazaki, M., Nakamura, Y. & Norisuye, T. Solution properties of polymacromonomers consisting of polystyrene. 1. Polymacromonomer consisting of polystyrene. light scattering characterization in cyclohexane. *Polym. J.* **31**, 193–198 (1999).

- (12) Terao, K., Nakamura, Y. & Norisuye, T. Solution properties of poly-macromonomers consisting of polystyrene. 2. Chain dimensions and stiffness in cyclohexane and toluene. *Macromolecules* **32**, 711–716 (1999).
- (13) Terao, K., Hokajo, T., Nakamura, Y. & Norisuye, T. Solution properties of polymacromonomers consisting of polystyrene. 3. Viscosity behavior in cyclohexane and toluene. *Macromolecules* **32**, 3690–3694 (1999).
- (14) Zhang, B., Grohn, F., Pedersen, J. S., Fischer, K. & Schmidt, M. Conformation of cylindrical brushes in solution: Effect of side chain length. *Macromolecules* **39**, 8440–8450 (2006).
- (15) Hokajo, T., Terao, K., Nakamura, Y. & Norisuye, T. Solution properties of polymacromonomers consisting of polystyrene. 5. Effect of side chain length on chain stiffness. *Polym. J.* **33**, 481–485 (2001).
- (16) Hokajo, T., Hanaoka, Y., Nakamura, Y. & Norisuye, T. Translational diffusion coefficient of polystyrene polymacromonomers. Dependence on side-chain length. *Polym. J.* **37**, 529–534 (2005).
- (17) Amitani, K., Terao, K., Nakamura, Y. & Norisuye, T. Small-angle X-ray scattering from polystyrene polymacromonomers in cyclohexane. *Polym. J.* **37**, 324–331 (2005).
- (18) Sugiyama, M., Nakamura, Y. & Norisuye, T. Dilute-solution properties of polystyrene polymacromonomer having side chains of over 100 monomeric units. *Polym. J.* **40**, 109–115 (2008).
- (19) Nakamura, Y. & Norisuye, T. Backbone stiffness of comb-branched polymers. *Polym. J.* **33**, 874–878 (2001).
- (20) Yamakawa, H. & Stockmayer, W. Statistical mechanics of wormlike chains. II. Excluded volume effects. *J. Chem. Phys.* **57**, 2843–2854 (1972).

- (21) Yamakawa, H. *Helical Wormlike Chains in Polymer Solutions* (Springer, Berlin 1997).
- (22) Fixman, M. & Skolnick, J. Polyelectrolyte excluded volume paradox. *Macromolecules* **11**, 863–867 (1978).
- (23) Yamakawa, H. *Modern Theory of Polymer Solutions* (Harper & Row, New York 1971).
- (24) Nakamura, Y., Norisuye, T. & Teramoto, A. Second and third virial coefficients for polystyrene in cyclohexane near the  $\theta$  point. *Macromolecules* **24**, 4904–4908 (1991).
- (25) Wang, M. C. & Uhlenbeck, G. E. On the theory of the brownian motion II. *Rev. Mod. Phys.* **17**, 323–342 (1945).
- (26) Cherayil, B. J., Douglas, J. F. & Freed, K. F. Effect of residual interactions on polymer properties near the theta point. *J. Chem. Phys.* **83**, 5293–5310 (1985).
- (27) Yamakawa, H. On the theory of the second virial coefficient for polymer chains. *Macromolecules* **25**, 1912–1916 (1992).
- (28) Barrett, A. J. Second osmotic virial coefficient for linear excluded volume polymers in the Domb-Joyce model. *Macromolecules* **18**, 196–200 (1985).
- (29) Abe, F., Einaga, Y., Yoshizaki, T. & Yamakawa, H. Excluded-volume effects on the mean-square radius of gyration of oligo- and polystyrenes in dilute solutions. *Macromolecules* **26**, 1884–1890 (1993).
- (30) Miyaki, Y., Einaga, Y. & Fujita, H. Excluded-volume effects in dilute polymer solutions. 7. Very high molecular weight polystyrene in benzene and cyclohexane. *Macromolecules* **11**, 1180–1186 (1978).



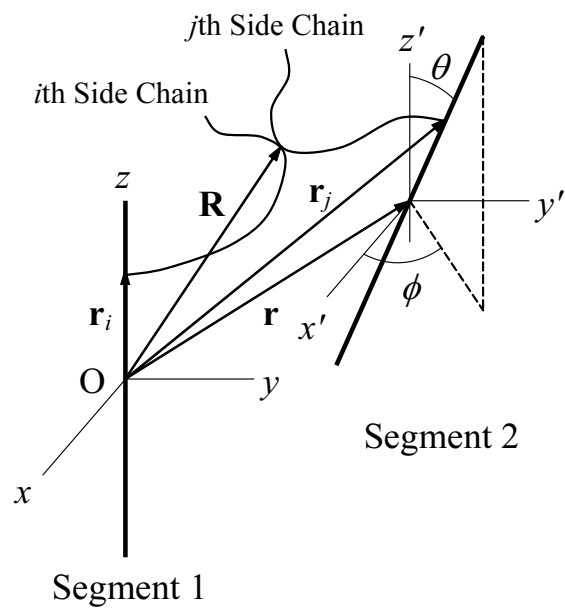


**Figure 1.** Coordinates of two brush-like segments.

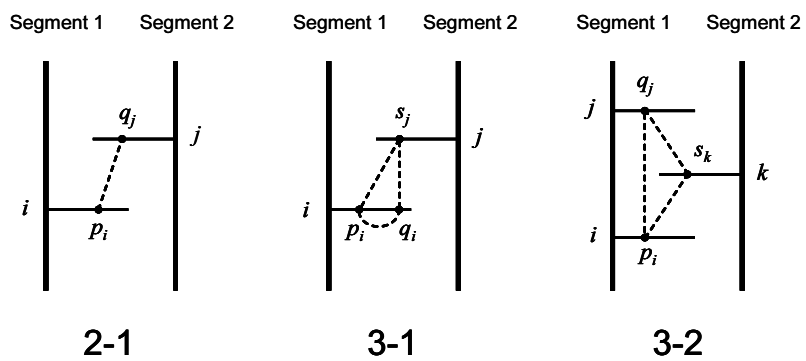


**Figure 2.** Diagrammatic representation of interactions among side chains. Thick and thin solid lines indicate the main and side chains, respectively. Dashed lines connect interacting segments.

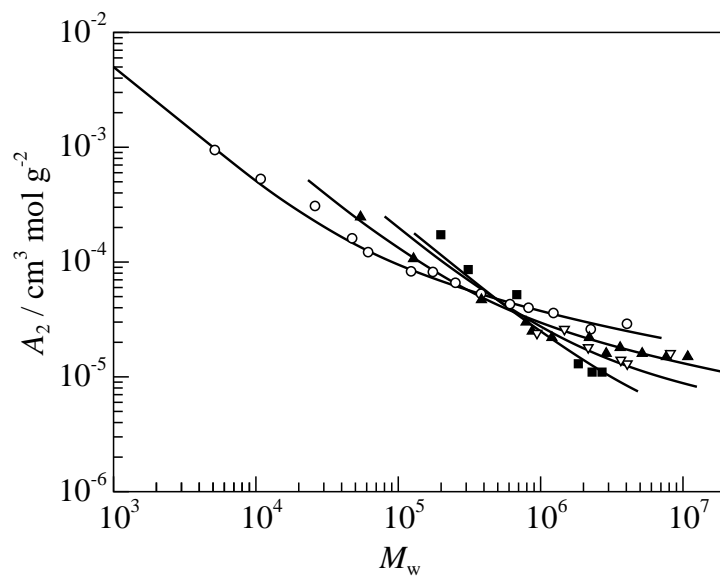


**Figure 3.** Molecular weight dependence of second virial coefficient for polystyrene polymacromonomers with different degree of polymerization of side chain in toluene: circles, F15;<sup>12</sup> filled triangles, F33;<sup>12</sup> unfilled triangles, F65;<sup>15</sup> squares, F110;<sup>18</sup> lines, calculated values.

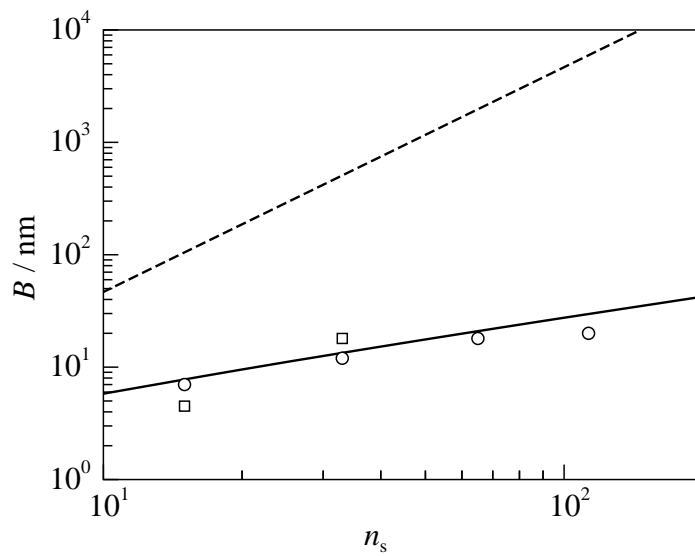


**Figure 4.**  $B$  for polystyrene polymacromonomers determined from the radius expansion factor (squares)<sup>12</sup> and the second virial coefficient (circles). Dashed and solid lines show calculated values from Eq (2) with (9) and (12), respectively.

**Table 1.** Molecular parameters for PS polymacromonomers in toluene at 15.0°C.

Sample	$n_s$	$M_L/10^3 \text{ nm}^{-1}$	$\lambda^{-1}/\text{nm}$	$a_{2,1}/\text{cm}^3 \text{ g}^{-1}$	$B / \text{nm}$	
					from $\langle S^2 \rangle$	from $A_2$
F15	15	6.2 <sup>a</sup>	16 <sup>a</sup>	5	4.5 <sup>a</sup>	7
F33	33	13.0 <sup>a</sup>	36 <sup>a</sup>	12	18 <sup>a</sup>	12
F65	65	25.0 <sup>b</sup>	75 <sup>b</sup>	20	—	18
F110	113	45.5 <sup>c</sup>	155 <sup>c</sup>	23	—	20

<sup>a</sup>Ref.12, <sup>b</sup>Ref.15, <sup>c</sup>Ref.18

**Table 2.** Calculated  $B$  for PS poly-macromonomers in cyclohexane at 34.5°C.

$n_s$	$B / \text{nm}$	
	from $v_{3-2}$	from $v_3^{\text{SD}}$
15	55	12
33	268	21
65	1038	33
113	3137	47